ORIGINAL RESEARCH

Role of the KRT7 Biomarker in Immune Infiltration and Paclitaxel Resistance in Ovarian Cancer

Shuai Wang, MM; Haiping Li, MM; Mojuan Li, MM; Xiaoguang Liu, MM; Shengquan Yu, MM; Hao Huang, BM; Xiaoyu Wang, PhD

ABSTRACT

Context • Paclitaxel (PTX) resistance is often associated with poor outcomes for patients with ovarian cancer (OC), but its mechanism is unknown. Clinicians are increasingly using immunotherapy in the management of OC, and the ability to assess tumor-immune interactions and identify effective, predictive, prognostic molecular biomarkers for OC is an urgent need.

Objective • The study intended to explore the potential tumorigenesis mechanisms to identify promising biomarkers and improve survival in OC patients.

Design • The research team performed a genetic analysis.

Setting • The study took place at First Affiliated Hospital of Jinan University, Guangzhou, Guangdong, China.

Outcome Measures • The research team: (1) obtained GSE66957 and GSE81778 gene expression profiles from the Gene Expression Omnibus (GEO) database and identified 468 differentially expressed genes (DEGs); (2) conducted functional enrichment analysis and constructed a protein-to-protein interaction (PPI) network; (3) identified the OC survival-related genes using the Gene Expression Profiling Interactive Analysis 2 (GEPIA2) webserver and compared those genes with upregulated DEGs to identify the core genes; (4) used GEPIA2 and the Kaplan-Meier plotter to explore the expression profiles and the prognostic values of the core genes in OC; (5) used the LinkOmics, Oncomine, and GEPIA2 web servers to perform co-expression analysis and explore functional networks correlated with keratin 7 (KRT7); (6) performed correlation analyses between KRT7, the six main types of tumor-infiltrating lymphocytes (TILs), and immune signatures, using the TIMER tool; and (7) subsequently detected the KRT7 expression in the cell lines IOSE80, A2780, A2780/PTX, ho8910, skov3, and ovcar3 using quantitative reverse transcription-polymerase chain reaction (RT-qPCR) technology.

Results • High expression levels of KRT7 were significantly correlated with progression-free survival (PFS) and poor overall survival (OS) for OC patients, with logrank $P = .0074$ and logrank $P = .014$, respectively. The expression levels of KRT7 were also significantly correlated with the infiltrated neutrophil levels ($r = 0.169$, $P = .0077$). The study identified neutrophils as potential predictors of survival in OC. Moreover, the expression levels of KRT7 in OC were positively correlated with 51 (31.68%) of the 161 immune gene markers. The RT-qPCR analyses revealed a high expression of KRT7 in the paclitaxel-resistant OC cell line.

Conclusions • KRT7 is correlated with immune infiltration and paclitaxel resistance in OC patients. Therefore, clinicians could use KRT7 as a prognostic marker and a target in the development of new drugs. (*Altern Ther Health Med.* 2023;29(5):132-140).

Shuai Wang, MM, Associate Chief Physician, Department of Obstetrics and Gynecology, the First Affiliated Hospital of Jinan University, Guangzhou, Guangdong, China, and Department of Obstetrics and Gynecology, the Sixth Affiliated Hospital, South China University of Technology, Foshan, Guangdong, China. **Haiping Li,** MM, Attending Doctor, Department of Gynecology, Guangdong Women and Children Hospital, Guangzhou, Guangdong, China. **Mojuan Li,** MM, Associate Chief Physician; **Shengquan Yu,** MM, Resident Doctor; and **Hao Huang,** BM, Chief Physician; Department of Obstetrics and Gynecology, the Sixth Affiliated Hospital, South China University of Technology, Foshan, Guangdong, China. **Xiaoguang Liu,** MM, Attending Doctor, Department of Gynecology, Nanjing Maternal and Child Health Care Hospital, Obstetrics and Gynecology Hospital Affiliated to Nanjing Medical University, Nanjing, Jiangsu, China. **Xiaoyu Wang,** PhD, Chief Physician, Department of Obstetrics and Gynecology, the First Affiliated Hospital of Jinan University, Guangzhou, Guangdong, China.

Corresponding author: Xiaoyu Wang, PhD
E-mail: twxy@jnu.edu.cn
Corresponding author: Hao Huang, PhD
E-mail: 648978560@qq.com

Ovarian cancer (OC) is the fifth leading cause of cancer-associated deaths in women globally.[1] Approximately 70% of OC patients are in an advanced stage of the disease at diagnosis, because most symptoms experienced by patients aren't specific.[2] Late diagnosis of OC leads to a poor prognosis and high mortality, with a five-year survival rate below 40%.[3-5]

PTX Resistance

The first-line therapy for OC includes cytoreductive surgery and combined paclitaxel-based chemotherapy.[6] Paclitaxel (PTX) resistance is a critical challenge in OC treatment.[7] Huang et al found that several biomarkers were associated with resistance to cytotoxic chemotherapy in OC, including X-inactive specific transcript (XIST), which is associated with paclitaxel-resistance.[8] Cai et al found that dysregulated miR-362-3p, miR-766-3p, and miR-6507-3p might confer paclitaxel resistance in the human lung carcinoma.[9] Li et al reported that paclitaxel resistance in hepatocellular carcinoma involved the "phosphatidylinositol 3 kinase-protein kinase B" (PI3K-Akt) pathway.[10]

However, researchers haven't found the mechanism that can reverse the PTX resistance. Therefore, it's imperative to clarify the molecular mechanism of PTX resistance in OC.

Differentially Expressed Genes

Clinicians are increasingly using immunotherapy in the management of OC, with promising results.[11] However, due to the specificity and high costs of these drugs, an urgent need exists to assess tumor-immune interactions and identify effective, predictive, prognostic molecular biomarkers for OC. Researchers are currently using gene chip technology to identify reliable, differentially expressed genes (DEGs) stored in public databases.[12,13]

Current Study

The study intended to explore the potential tumorigenesis mechanisms to identify promising biomarkers and improve survival in OC patients.

METHODS

Procedures

Outcome Measures. The research team: (1) obtained GSE66957 and GSE81778 gene expression profiles from the Gene Expression Omnibus (GEO) database and identified 468 differentially expressed genes (DEGs); (2) conducted functional enrichment analysis and constructed a protein-to-protein interaction (PPI) network; (3) identified the OC survival-related genes using the Gene Expression Profiling Interactive Analysis 2 (GEPIA2) webserver and compared those genes with upregulated DEGs to identify the core genes; (4) used GEPIA2 and the Kaplan-Meier plotter to explore the expression profiles and the prognostic values of the core genes in OC; (5) used the LinkOmics, Oncomine, and GEPIA2 web servers to perform co-expression analysis and explore functional networks correlated with keratin 7 (KRT7); (6) performed correlation analyses between KRT7, the six main types of tumor-infiltrating lymphocytes (TILs), and immune signatures, using the TIMER tool; and (7) subsequently detected the KRT7 expression in the cell lines IOSE80, A2780, A2780/PTX, ho8910, skov3, and ovcar3 using quantitative reverse transcription-polymerase chain reaction (RT-qPCR) technology.

Outcome Measures

Selection of core genes. The research team used online tools to explore DEGs in OC samples and normal ovarian (OV) samples in the GSE66957 and GSE81778 datasets[14] from the National Center for Biotechnology Information (NCBI) - Gene Expression Omnibus (GEO) database: (1) the GSE66957 dataset from the GPL15048 platform [Rosetta/Merck Human RSTA Custom Affymetrix 2.0 microarray (HuRSTA_2a520709.CDF)] and (2) the GSE81778 dataset from the GPL14951 platform [Illumina HumanHT-12 WG-DASL V4.0 R2 expression gene chip]. We select the dataset by keyword "ovarian cancer" and choose the dataset whiche contains "ovarian cancer" and "ovarian normal samples".

The team: (1) determined the DEGs that overlapped between the GSE66957 and GSE81778 datasets using the dplyr, openxlsx, data.table, and VennDiagram packages available in the R software, version 4.0.2 (R Core Team, Vienna, Austria), and (2) chose DEGs with a log fold change (FC) of two and a corrected $P < .05$ as the overlapping DEGs.

The Gene Expression Profiling Interactive Analysis 2 (GEPIA2) web tool contains the RNA-sequencing expression data of 9736 tumors and 8587 normal samples from the Genotype-Tissue Expression (GTEx) and the Cancer Genome Atlas (TCGA) databases.[15] The research team retrieved the top 500 genes significantly related to survival in the OC dataset from the GEPIA2 database and compared those genes to the upregulated, overlapping DEGs, using the jvenn online tools.[16]

Protein-to-protein interaction (PPI) network and functional enrichment analysis. The research team used the STRING database to construct a PPI network of overlapped DEGs.[17] Interactions with a combined score above 0.4 were considered to be statistically significant.

The Web-based Gene Set Analysis Toolkit (WebGestalt) is a suite of tools used for functional enrichment analysis of biological data.[18] The research team used WebGestalt for enrichment analysis of overlapping DEGs under the following terms: biological process (BP), molecular function (MF), and cellular component (CC).

For the analysis using the Kyoto Encyclopedia of Genes and Genomes (KEGG) pathway, the research team chose a $P < .05$ as being statistically significant. The team visualized the findings using the ggplot2 and dplyr packages available on the R software version 4.0.2 (Hadley Wickham). The team considered a false discovery rate (FDR) of <.01 and gene counts of ≥10 to be statistically significant.

Analysis of selected core genes. The research team: (1) validated the gene expression and prognostic value of the

five core genes using the Gene Expression Profiling Interactive Analysis 2 (GEPIA2) database; (2) validated the prognostic value of the core genes again using the Kaplan-Meier plotter[19]; and (3) validated the overexpression of the keratin 7 (KRT7) gene in OC again using the Oncomine webserver.[20]

Analysis using LinkedOmics and GEPIA2 databases. LinkedOmics is a public database containing multi-omics data from 32 cancer types from the Cancer Genome Atlas (TCGA).[21] The research team: (1) used the LinkFinder module in LinkedOmics for Pearson correlation analysis on KRT7 co-expression, and (2) presented the data using heatmaps, scatter plots, or volcano plots. The team generated the survival heatmaps of significantly expressed genes using GEPIA213.

Correlation between KRT7 and infiltrating immune cells. The research team used the Tumor Immune Estimation Resource (TIMER) tool to evaluate the immune infiltration in different cancers systematically.[22] The team performed correlation analyses between the expression of KRT7 and levels of six types of immune cells in OC, including dendritic cells, B cells, cluster of differentiation 8+ (CD8+) T cells, CD4+ T cells, macrophages, and neutrophils, using the TIMER tool.

The team then: (1) explored the prognostic value of the six immune-cell infiltrates in OC using a Kaplan-Meier analysis and (2) investigated the effects of KRT7 and the immune-cell infiltrates on overall survival (OS) using multivariate Cox analysis.

Relationship between KRT7 and immune signatures. TISIDB is a web portal used to analyze tumor and immune system interactions[23] and has various immune gene signatures categorized based on the type of immune cells or their function. The research team: (1) retrieved the gene signatures of the six tumor-infiltrating lymphocytes (TILs), including dendritic cells, B cells, CD8+ T cells, CD4+ T cells, macrophages, and neutrophils and (2) performed a correlation analysis of KRT7 and the gene signatures using the purity-corrected partial Spearman method available in the Correlation module in TIMER.

Cell lines and cell culture. The research team: (1) obtained the OV cell line IOSE80, and the OC cell lines A2780, A2780/PTX, ho8910, skov3, and ovcar3 from the Shanghai Institute for Biological Sciences of the Chinese Academy of Sciences (Shanghai, China); (2) cultured the cells in Dulbecco's Modified Eagle's Limiting Medium (DMEM) from Thermo Fisher Scientific (Waltham, MA, USA) with 10% fetal bovine serum (FBS) from Thermo Fisher Scientific (Waltham, MA, USA) in a 5% carbon dioxide humidified incubator (Esco Lifesciences Group, Singapore) at 37°C; (3) extracted the total RNA using the Trizol reagent (Invitrogen, Carlsbad, CA, USA), according to the manufacturer's instructions; (4) performed quantitative reverse transcription-polymerase chain reaction (RT-qPCR) with Power SYBR Green PCR Master Mix (TransGen Biotech, Beijing, China) on the ABI 7500 fast real-time PCR system (Applied Biosystems, Waltham, MA, USA); (5) first performed the amplification reaction procedure at 95°C for 10 minutes, then at 95°C for 15 seconds, and finally at 60°C for one minute for 40 cycles; (5) applied glyceraldehyde 3-phosphate dehydrogenase (GAPDH) as an internal control for mRNA; (6) calculated the relative expression level of mRNA using the 2^(–delta delta CT) method and the primer sequences: KRT7: F'-TCCGCGAGGTCACCATTAAC, R'-GCTCTGTC AACTCCGTCTCAT. GAPDH-F'-GGGAAACTGTGGCGT GAT, R'-GTGGTCGTTGAGGGCAAT; and (7) repeated the experiments at least three times and analyzed the samples in triplicate.

Statistical Analysis

The research team used the GraphPad Prism6 software (GraphPad Software, La Jolla, CA, USA) to analyze and present the data. The team expressed measurement data as means ± standard deviations (SDs) and performed a two-sided Student's *t* test to compare KRT7 expression levels between the normal OV and OC cell lines. $P < .05$ was statistically significant for all bioinformatics tests described above.

RESULTS

DEGs in OC Cells and Core Genes

For the GSE66957 dataset, the GEO2R platform contained tissue samples of 57 OC and 12 normal OV cells. For the GSE81778 dataset, the GPL14951 platform contained tissue samples of 19 OC and 5 OV samples.

The GSE66957 and GSE81778 datasets provided 1004 and 585 DEGs, respectively, and 468 were overlapping DEGs. Out of the 468 DEGs, 160 genes were upregulated, and 308 genes were downregulated in OC tissues compared to normal OV tissues (Figure 1A).

The GEPIA2 web portal provided the top 500, most-significant, survival-associated genes in OC. Figure 1B shows the comparison of them with 160 upregulated overlapping DEGs, with the intersecting genes identified as the core genes, including sodium channel epithelial 1 subunit alpha-human (SCNN1A), secretory leukocyte peptidase inhibitor (SLPI), KRT7, receptor interacting serine/threonine kinase 4-human (RIPK4), and lysine deficient protein kinase 1 (WNK1).

The construction of the PPI network used 459 DEGs, consisting of 537 edges and 459 nodes. The PPI network construction didn't use nine genes of the 468 DEGs (Figure 1C) because they were less correlated with the main PPI network.

Bioinformatics Analyses

For the BP analysis of the overlapping DEGs, Figure 2A shows that the Gene Ontology (GO) functional-enrichment analysis found the DEGs to be significantly implicated in the response to endogenous stimulus (logrank $P = 15.43$), cell migration (logrank $P = 15.18$), tissue development (logrank $P = 14.84$), cell motility (logrank $P = 14.84$), localization of cells (logrank $P = 14.84$), cellular response to endogenous stimulus (logrank $P = 14.44$), circulatory-system development (logrank $P = 14.65$), locomotion (logrank $P = 13.87$), anatomical

Figure 1. Selection of Core Genes and Bioinformatics Analyses of DEGs. Figure 1A shows the authentication of the 468 common DEGs in the GSE66957 and GSE81778 datasets. The Venn diagram compares the upregulated genes (n = 160) and downregulated genes (n = 308) in OC tissues with normal OV tissues. Figure 1B shows the comparison of the 160 upregulated genes to the 500 most-significant, survival-associated genes in OC according to the GEPIA2 web-based server. The comparison identified five intersecting genes as the core genes. Figure 1C shows the 459 DEGs that the research team used to construct a PPI network consisting of 537 edges and 459 nodes. The nodes indicate the genes, and the varying line thicknesses correspond to the strength of the data support.

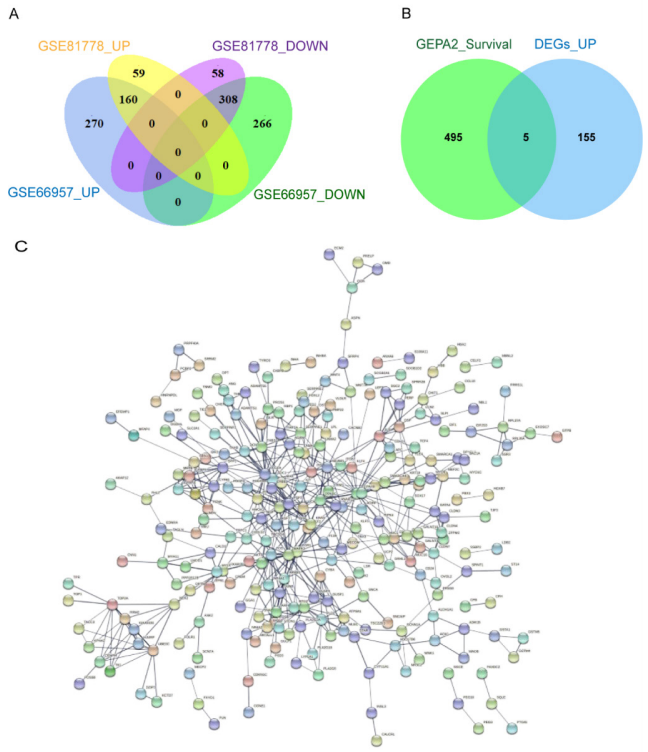

Abbreviations: DEGs, differentially expressed genes; GSE, Genomic Spatial Event database; OC, ovarian cancer; OV, ovarian; PPI, protein-to-protein interaction.

Figure 2. GO and KEGG Analysis of the Overlapping DEGs in OC. Figure 2A shows the biological process (BP); Figure 2B shows the cellular component (CC); Figure 2C shows the molecular function (MF); and Figure 2D shows the KEGG pathway.

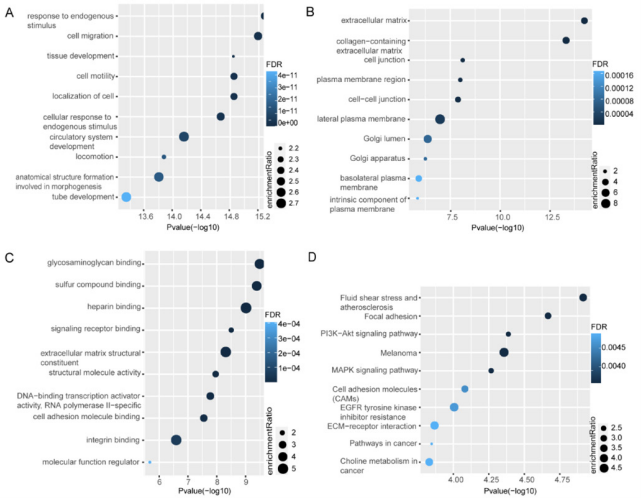

*$P < .05$, indicating that the overlapping DEGs were significantly implicated in the biological processes (BP), molecular functions (MF), cellular components (CC), and the KEGG pathway

Abbreviations: ECM, extracellular matrix; EFGR, epidermal growth factor receptor; FDR, false discovery rate; GO, gene ontology; KEGG, Kyoto Encyclopedia of Genes and Genomes; MAPK, mitogen-activated protein kinase; OC, ovarian cancer; P13K-Akt, phosphatidylinositol 3 kinase-protein kinase B.

structure formation involved in morphogenesis (logrank $P = 13.78$), and tube development (logrank $P = 13.33$).

For the CC analysis of the overlapping DEGs, Figure 2B shows significant enrichment in the extracellular matrix (ECM; logrank $P = 14.21$), collagen-containing ECM (logrank $P = 13.29$), cell junction (logrank $P = 8.11$), plasma membrane region (logrank $P = 7.98$), cell-to-cell junction (logrank $P = 7.86$), lateral plasma membrane (logrank $P = 6.93$), Golgi lumen (logrank $P = 6.32$), and Golgi apparatus (logrank $P = 6.32$). Additionally, enrichment also occurred in the basolateral plasma membrane (logrank $P = 6.22$) and the intrinsic component of plasma membrane (logrank $P = 5.69$).

For the MF analysis of the overlapping DEGs, Figure 2C shows that functional-enrichment analysis found the DEGs to be significantly implicated in the response to glycosaminoglycan binding (logrank $P = 9.45$), sulfur compound binding (logrank $P = 9.35$), heparin-binding (logrank $P = 8.97$), signaling receptor binding (logrank $P = 8.48$), ECM structural constituent (logrank $P = 8.27$), structural molecule activity (logrank $P = 7.93$), DNA-binding transcription activator activity, RNA polymerase II-specific (logrank $P = 7.74$), cell adhesion molecule (CAM) binding (logrank $P = 7.52$), integrin binding (logrank $P = 6.55$), and molecular function regulator(logrank $P = 5.66$).

Furthermore, Figure 2D shows that the KEGG analysis implicated the DEGs in fluid shear stress and atherosclerosis (logrank $P = 4.91$), focal adhesion (logrank $P = 4.66$), the PI3K-Akt transduction pathway (logrank $P = 4.38$), melanoma (logrank $P = 4.35$), the mitogen-activated protein kinase (MAPK) signaling pathway (logrank $P = 4.26$), CAMs (logrank $P = 4.08$), epidermal growth factor receptor (EGFR)-tyrosine kinase inhibitor resistance (logrank $P = 4.00$), ECM-receptor interaction (logrank $P = 3.86$), and cancer and choline metabolic pathways (logrank $P = 3.82$).

Figure 3. The Expression Levels and Survival Analysis of the Core Genes Using the GEPIA2 (N = 212). Figures 3A to 3E compare the differences in expression levels of the core genes between OC tissues and normal tissues. The research team analyzed five core genes using the GEPIA online database. Figures 3F to 3J illustrate the results of the Kaplan–Meier OS analysis of the five core genes in OC. The research team plotted the survival curves using the GEPIA web server. Five core genes were associated with significantly poor survival in OC patients if the five core genes were highly expressed. The figures shows the genes in the cohort with high expression in red, while the blue line indicates the low-expression cohort. The dotted lines represent the survival curves, and the solid line represents the 95% confidence interval. The team calculated the *P* values using log-rank statistics.

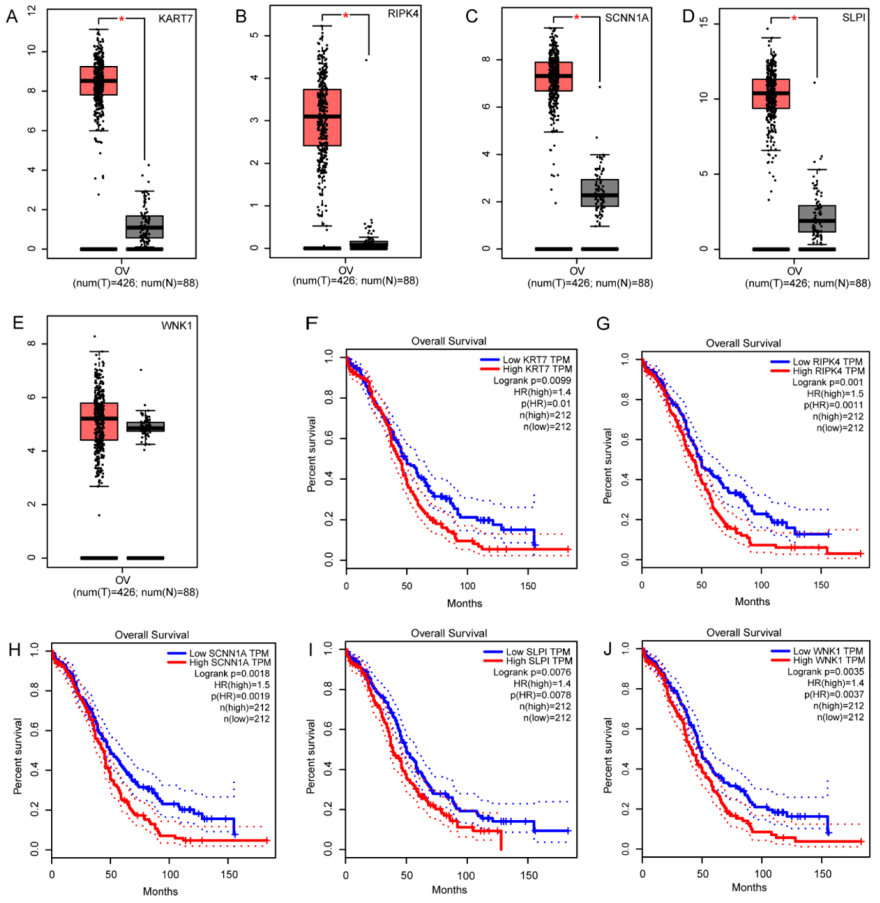

*$P < .05$, indicating that four out of five genes—SCNN1A, SLPI, KRT7, and RIPK4—had significantly higher expression levels in OC when compared with normal OV tissue and all five genes were associated with significantly poorer survival for OC patients than for women without OC

Abbreviations: GEPIA2, Gene Expression Profiling Interactive Analysis 2; HR, hazard ratio; KRT7, keratin 7; OC, ovarian cancer; OS, overall survival; OV, ovarian; RIPK4, receptor interacting serine/threonine kinase 4 (human); SCNN1A, sodium channel epithelial 1 subunit alpha (human); SLPI, secretory leukocyte peptidase inhibitor; TPM, transcript per million; WNK1, lysine deficient protein kinase 1.

Selected Core Genes

Figures 3A to 3E show that four out of five of the core genes—KRT7, RIPK4, SCNN1A, and SLPI—were significantly highly expressed in OC samples compared with the levels in normal OV samples ($P < .01$), but WNK1 wasn't ($P < .01$). Figures 3F to 3J show that the expression levels and OC survival information for the five core genes—KRT7 (logrank $P = .01$), RIPK4 (logrank $P = .0011$), SCNN1A (logrank $P = .0019$), SLPI (logrank $P = .0078$), and WNK1 (logrank $P = .0037$)—were associated with significantly poorer survival for OC patients than for women without OC.

Figures 4A to 4D show that the OS in patients with the KRT7 (logrank $P = 0.014$) and SLPI (logrank $P = .0024$) genes was significantly shorter than for the SCNN1A (logrank $P = .032$) and RIPK4 logrank ($P = .056$) genes. Figures 4E to 4H show that the KRT7 (logrank $P = .0074$) gene was significantly correlated with poorer progression-free survival (PFS) than the SLPI (logrank $P = .06$), RIPK4 (logrank $P = .0044$), and SCNN1A (logrank $P = .10$) genes.

Figure 4. The Survival Analysis of Core Genes Using the Kaplan Meier Online Plotter Tool. The research team used the online Kaplan Meier plotter tool to calculate the PFS and OS of the four core genes. The OS in the SLPI and KRT7 genes was significantly poorer than for the SCNN1A and RIPK4 genes. The KRT7 (Figures 4A and 4E) was correlated with significantly worse PFS, but the RIPK4 (Figures 4B and 4F), SCNN1A (Figures 4C and 4G), and SLPI (Figures 4D and 4H) genes weren't. A log-rank of $p < .05$ was considered to be statistically significant.

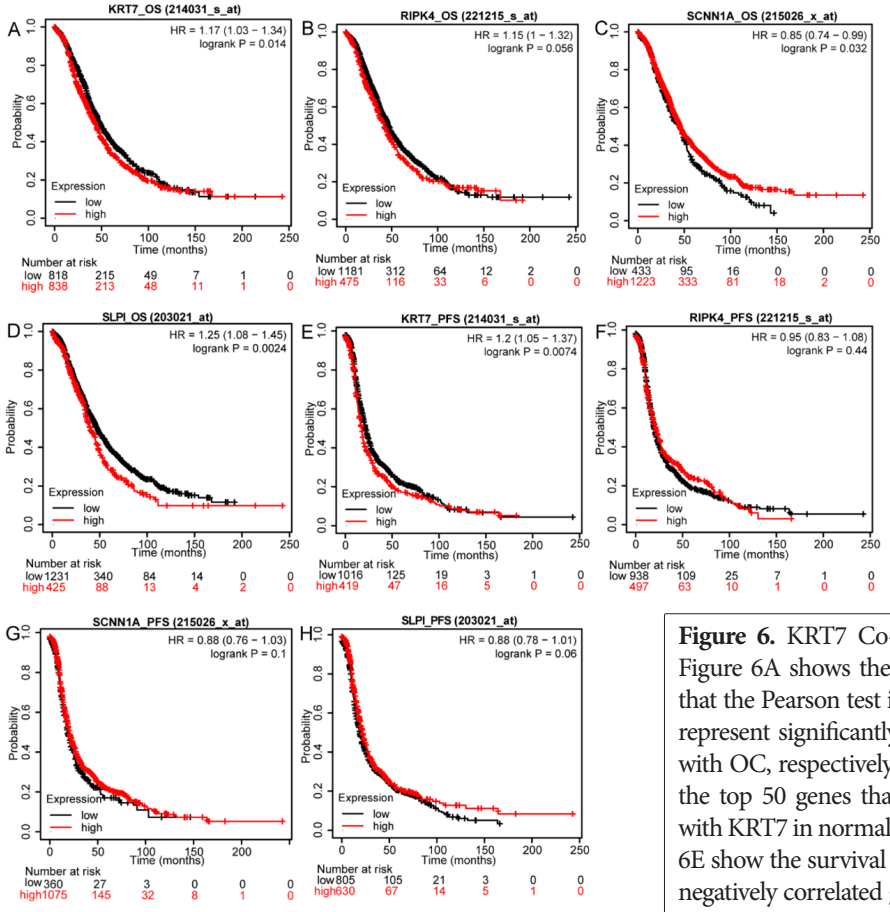

*$P < .05$, indicating that the OS in patients with the KRT7 and SLPI genes was significantly shorter than for the SCNN1A and RIPK4 logrank genes and that the KRT7 gene was significantly correlated with poorer PFS than the other four genes

Abbreviations: HR, hazard ratio; KRT7, keratin 7; OS, overall survival; PFS, progression-free survival; RIPK4, receptor interacting serine/threonine kinase 4 (human); SCNN1A, sodium channel epithelial 1 subunit alpha (human); SLPI, secretory leukocyte peptidase inhibitor.

The analysis using Oncomine indicated a high expression of KRT7 in OC samples compared with normal OV samples (Figure 5).

KRT7 Co-expression Networks

Figure 6A shows the profile analysis of KRT7 co-expression in OC. The blue dots in Figures 6B and 6C indicate a positive relationship with KRT7 for 3012 genes,

Figure 5. Oncomine Analysis and RT-qPCR Validation of KRT7 in OV and OC cell lines. The figure shows the Oncomine analysis of KRT7 in six histological subtypes of OC versus normal tissue.

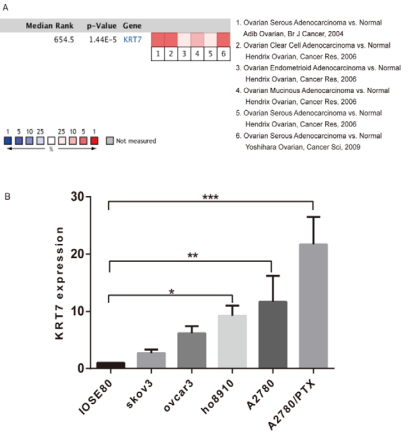

Abbreviations: KRT7, keratin 7; OC, ovarian cancer; OV, ovarian; PTX, paclitaxel; RT-qPCR, quantitative reverse transcription-polymerase chain reaction.

Figure 6. KRT7 Co-expression Genes in OC (LinkedOmics). Figure 6A shows the global genes highly correlated with KRT7 that the Pearson test in LUAD identified. The red and green dots represent significantly positively and negatively correlated genes with OC, respectively. The heatmaps in Figures 6B and 6C show the top 50 genes that were positively and negatively correlated with KRT7 in normal OV tissue. The heatmaps in Figures 6D and 6E show the survival of the top 50 genes that were positively and negatively correlated genes with KRT7 in OC, as hazard ratios in the logarithmic scale (log10) for different genes. The red and blue blocks denote higher and lower risks, respectively. The rectangles with the bold outlines indicate the significant unfavorable and favorable results ($P < .05$) in the prognostic analyses.

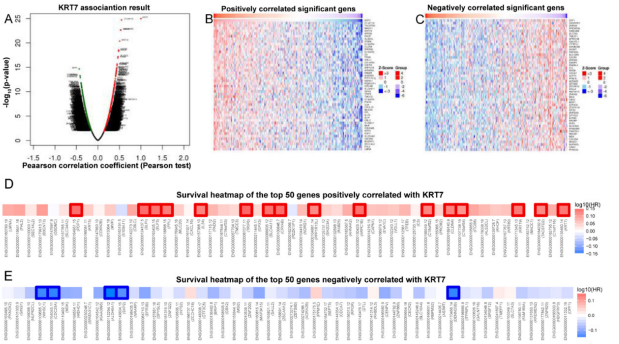

*$P < .05$, indicating that the top 50 genes were significantly negatively and positively correlated with KRT7

Abbreviations: KRT7, keratin 7; LUAD, lung adenocarcinoma; OC, ovarian cancer; OV, ovarian.

Figure 7. Correlation Analysis Between KRT7 Expression and the Six Types of Infiltrating Immune Cells in OC. Figure 7A shows the correlation of the KRT7 expression with the six cell types, obtained using TIMER (purity-corrected Spearman test).[20] The KRT7 expression was correlated with levels of macrophages, neutrophils, and CD8+ T cells. Figure 7B shows the OS overall survival curve for each of the six cell types, obtained using the Kaplan-Meier estimator from TIMER.[20] The research team compared the survival differences between the high and low cell types according to the median and identified only neutrophils as potential predictors of the outcomes in OC.

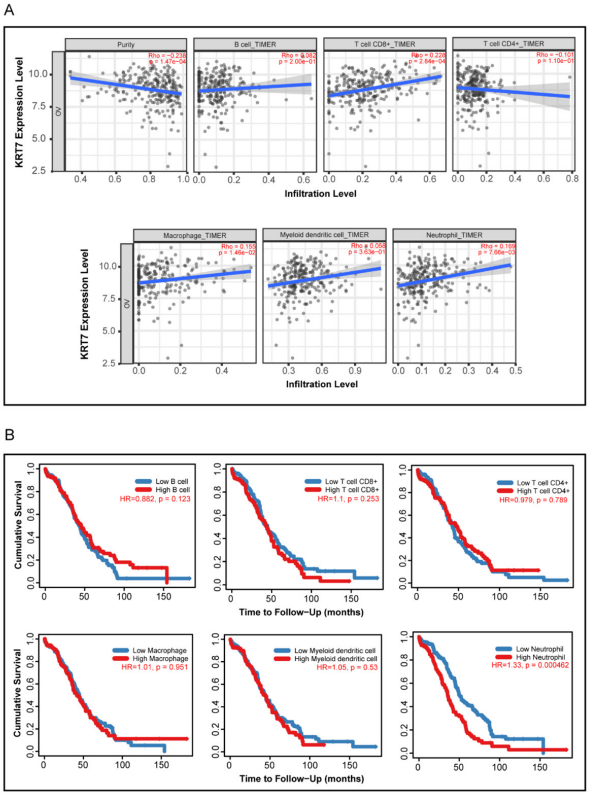

*$P < .05$, indicating that KRT7 expression was significantly correlated with levels of macrophages, neutrophils, and CD8+ T cells

Abbreviations: CD8, cluster of differentiation 8; HR, hazard ratio; KRT7, keratin 7; OC, ovarian cancer; OS, overall survival; TIMER, Tumor Immune Estimation Resource

and the red dots indicate a negative relationship with KRT7 for 5059 genes ($P < .05$).

Figures 6D and 6E show heatmaps of the top 50 genes, and the genes were negatively and positively correlated with KRT7. Analysis of the expression of KRT7 showed a significant positive correlation with the expression of some genes, including: (1) the chromosome 1 open reading frame 116 (C1orf116) gene—positive rank #1, r = 0.551, and $P = 1.96 \times 10^{-25}$; (2) the "tumor associated calcium signal transducer 2" (TACSTD2) gene—r = 0.531 and $P = 2.10 \times 10^{-23}$; and (3) the metastasis-associated in colon cancer 1 (MACC1) gene—r = 0.530 and $P = 2.43 \times 10^{-23}$.

Figure 6D shows that a high hazard ratio (HR) existed for 16 out of the 50 positively correlated genes ($P < .05$), and they were therefore high-risk markers for OC. Figure 6E shows that five out of the top 50 negatively correlated genes had a low HR ($P < .05$).

KRT7 Expression and Infiltrating Immune Cells

Figure 7A shows that the correlation analysis between KRT7 expression and the six main infiltrating immune cells in OC found that KRT7 expression was significantly correlated with levels of macrophages (r = 0.155, $P = .0146$), neutrophils (r = 0.169, $P = .00766$), and CD8+ T cells (r = 0.228, $P = .000284$). The Kaplan-Meier analysis showed that only neutrophils ($P = .000462$) were potential predictors of survival in OC (Figure 7B).

KRT7 Levels and Immune Markers

Table 1 provides the full analysis evaluating the crosstalk between KRT7 and several immune-specific genes in the six TILs and a summary of the findings. Of the 161 immune-marker genes, the KRT7 expression in OC was significantly linked to 51 (31.68%). Of the 161, 26 (16.15%) were positively correlated with KRT7 expression, and 25 (15.53%) were negatively correlated with KRT7 expression.

Correlation analysis was performed to explore the crosstalk between KRT7 and several immune specific genes of the 6 TILs (Table S2). The contents of Table S2 was summarized as Table 1. The findings showed that *KRT7* expression in OC was markedly linked to 31.68% (51/161) of the total immune marker genes (Table 1). Notably, 26 out of 161 (16.15%) immune markers were positively correlated with *KRT7* expression, whereas, 25 out of 161 (15.53%) immune markers were negatively correlated with *KRT7* expression (Table 1). The HRH1 (r=0.314376, $P = .000000409$), TNFAIP2 (r = 0.282506, $P = .00000595$), and STEAP4 (r = 0.238554, $P = .000144466$) (Table S2) were the top 3 marker genes positively correlated with KRT7, whereas *CETN3* (r = -0.233973866, $P = .000195076$), *NUF2* (r = -0.226413447, $P = .000316203$), and *GNG7* (r = -0.221430165, $P = .000431014$) (Table S2) were the top 3 marker genes negatively correlated with *KRT7*.

Neutrophil cell infiltration is the main mechanism through which *KRT7* exhibits its prognostic role in our study. Therefore, further correlation analysis was performed between *KRT7* and Neutrophil cell marker genes. Purity-corrected partial Spearman's correlation between KRT7 and Neutrophil cell markers is presented in table (Table S2). *KRT7* was positively related to *STEAP4* (r = 0.238554270, $P = .000144466$), *VNN3* (r = 0.182521012, p-value = 0.003852954), and *CHST15* (r = 0.182127745, $P = .00393129$) in neutrophil cells.

Validation of KRT7 in OV and OC cell lines

The Rt-qPCR analysis detected higher KRT7 expression levels in all five evaluated OC cell lines compared with the

Table 1. Correlation Analysis Between KRT7 and Six Different Types of Immune Cells Markers in OC

	Activated B Cell n = 24 n (%)	CD4+ T Cell n = 25 n (%)	CD8+ T Cell n = 26 n (%)	Activated Dendritic Cell n = 35 n (%)	Macrophage n = 33 n (%)	Neutrophil n = 18 n (%)	Six Immune Cells n = 161 n (%)
Positive Correlations	4 (16.67)	2 (8.00)	4 (15.38)	10 (28.57)	3 (9.09)	3 (16.67)	26 (16.15)
Negative Correlations	3 (12.50)	9 (36.00)	7 (26.92)	2 (5.71)	3 (9.09)	1 (5.56)	25 (15.53)
Total Proportion	7 (29.17)	11 (44.00)	11 (42.31)	12 (34.29)	6 (18.18)	4 (22.22)	51 (31.68)

Figure 8. Oncomine Analysis and RT-qPCR Validation of KRT7 in OV and OC cell lines. The figure shows the upregulated expression of KRT7 in five OC cell lines, including skov3, ovcar3 ho8910, A2780, and A2780/PTX. However, compared with the normal OV cell line IOSE80, only the differences in KRT7 expression in the A2780/PTX, A2780, and ho8910 cell lines were statistically significant.

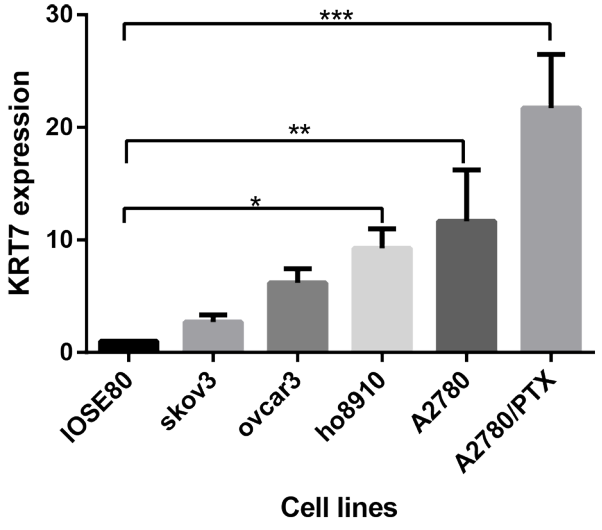

*$P < .05$, indicating that the expression of KRT7 was significantly higher in the OC cell line ho8910 than that in the normal OV cell line IOSE80

**$P < .05$, indicating that the expression of KRT7 was significantly higher in the OC cell line A2780 than that in the normal OV cell line IOSE80

***$P < .05$, indicating that the expression of KRT7 was significantly higher in the OC cell line A2780/PTX than that in the normal OV cell line IOSE80

normal OV cell lines. To further verify the expression of the KRT7 in OV and OC cell lines, the research team detected KRT7 expression in IOSE80, A2780, A2780/PTX, ho8910, skov3, and ovcar3. The expression of KRT7 was upregulated in five OC cell lines compared to the OV cell line IOSE80, and the upregulation was statistically significant for the comparison of the normal OV cell line IOSE80 and the OC cell lines ho8910, A2780, A2780/PTX, with A2780/PTX having the highest level of significance (Figure 8).

DISCUSSION

The current study used bioinformatics analyses that revealed 468 overlapping DEGs with aberrant expression in OC cells when compared with normal OV tissues, and it used a novel way to find the core genes. The research team compared survival-associated genes from GEPIA2 with 160 upregulated overlapping DEGs, and five intersecting core genes, including SCNN1A, SLPI, KRT7, RIPK4, and WNK1, were associated with survival and were overexpressed in OC.

The current study's analysis of the core genes in different independent data sets showed that only high expression of KRT7 was significantly correlated with PFS and OS in OC. WNK1 wasn't highly expressed in OC samples when compared with the levels in normal OV samples. Therefore, the research team selected KRT7 for subsequent immune analysis and RT-qPCR analysis as its role in OC was still unknown to the team's knowledge.

The current study explored biological functions and signaling pathways associated with the overlapped DEGs. For BP, overlapped DEGs were significantly enriched in response to an endogenous stimulus.

The current study's analysis using LinkedOmics showed that C1orf116, TACSTD2, MACC1 were the top three genes significantly positively correlated with KRT7. Several studies previously found that all three genes were associated with cancer prognosis.[24-26] The findings of the present study indicated that KRT7 expression levels were significantly correlated with infiltrating neutrophils. Moreover, Kaplan-Meier analysis showed that neutrophils were potential predictors of the outcome of OC. This implies that neutrophil infiltration in tumor cells is a critical factor related to the prognostic value of KRT7. Cheng et al reported that infiltrating neutrophils play a role in the mechanism of cisplatin resistance in lung cancer.[27]

The current study's correlation analyses between KRT7 and immune markers showed that four out of 18 neutrophil marker genes (22.22%) were positively correlated with KRT7 expression, including STEAP4. Tamura previously found that STEAP4 binds to focal adhesion kinase (FAK) to regulate its activation, thus affecting cell growth,[28] and this mechanism may influence cancer progression.

Li et al reported that expression of the KRT7 gene primarily occurs in epithelial tumors.[29] The current study further validated the expression of KRT7 in normal OV and OC cell lines using RT-qPCR technology. The research team observed a significantly higher expression of KRT7 in the paclitaxel-resistant OC cell line A2780/PTX compared to

paclitaxel-sensitive OC cell lines A2780, ho8910, skov3, and ovcar3 for the first time.

With only a few studies having explored the effects of the biological function of KRT7 in OC and its implication on prognosis,[30] the present study sought to perform a comprehensive and multi-angle analysis of KRT7 using various databases to explore the role of KRT7 in OC. The research team explored the correlation between KRT7 expression and different immune cells as well as immune genes linked to KRT7 that affect the prognosis of OC.

The current study first confirmed the high expression of KRT7 in the paclitaxel-resistant OC cell line. In addition, the bioinformatics analysis also observed mechanisms associated with drug resistance. These results provide some theoretical support for the use of KRT7 as a potential diagnostic biomarker and molecular target in the development of new OC chemotherapy drugs.

The current study, through using public databases, found that KRT7 was associated with paclitaxel resistance, being highly expressed in the paclitaxel-resistant ovarian cancer cell line A2780/PTX, and immunotherapy in OC and played a significant role in OC progression. The outcomes of the study help to identify new biological targets and strategies for the diagnosis, treatment, and prognosis assessment of OC.

This study had some limitations. The research team didn't validate the findings through sufficient experimental studies. Furthermore, the study didn't fully explore the underlying mechanism of the effects of KRT7 on OC progression and tumorigenesis. Therefore, the team should conduct further studies to explore the function and possible mechanisms of KRT7 in OC, which is a new direction in OC research

CONCLUSIONS

KRT7 is correlated with immune infiltration and paclitaxel resistance in OC patients. Therefore, clinicians could use KRT7 as a prognostic marker and a target in the development of new drugs.

AUTHOR CONTRIBUTIONS

Shuai Wang, MM, and Haiping Li, MM, contributed equally.

AUTHORS' DISCLOSURE STATEMENT

The National Natural Science Foundation of China (Grant No. 81901555), Science and Technology Innovation of Foshan (Grant No. 1920001001153), and Science and Technology Innovation of Foshan (Grant No.FS0AA-KJ218-1301-0037) funded the study. The funding bodies had no role in either the design of the study; the collection, analysis, and interpretation of data; or the writing of the manuscript. The authors declare that they have no conflict of interests related to the study.

AVAILABILITY OF DATA AND MATERIALS

The datasets used during the current study can be accessed through the following GEO database (open source): GSE66957: https://www.ncbi.nlm.nih.gov/geo/query/acc.cgi?acc=GSE66957; GSE81778: https://www.ncbi.nlm.nih.gov/geo/query/acc.cgi?acc=GSE81778

REFERENCES

1. Siegel RL, Miller KD, Jemal A. Cancer Statistics, 2017. *CA Cancer J Clin*. 2017;67(1):7-30. doi:10.3322/caac.21387
2. Maringe C, Walters S, Butler J, et al; ICBP Module 1 Working Group. Stage at diagnosis and ovarian cancer survival: evidence from the International Cancer Benchmarking Partnership. *Gynecol Oncol*. 2012;127(1):75-82. doi:10.1016/j.ygyno.2012.06.033
3. Allemani C, Weir HK, Carreira H, et al; CONCORD Working Group. Global surveillance of cancer survival 1995-2009: analysis of individual data for 25,676,887 patients from 279 population-based registries in 67 countries (CONCORD-2). *Lancet*. 2015;385(9972):977-1010. doi:10.1016/S0140-6736(14)62038-9
4. Jayson GC, Kohn EC, Kitchener HC, Ledermann JA. Ovarian cancer. *Lancet*. 2014;384(9951):1376-1388. doi:10.1016/S0140-6736(13)62146-7
5. Lheureux S, Gourley C, Vergote I, Oza AM. Epithelial ovarian cancer. *Lancet*. 2019;393(10177):1240-1253. doi:10.1016/S0140-6736(18)32552-2
6. Tsujioka H, Yotsumoto F, Hikita S, Ueda T, Kuroki M, Miyamoto S. Targeting the heparin-binding epidermal growth factor-like growth factor in ovarian cancer therapy. *Curr Opin Obstet Gynecol*. 2011;23(1):24-30. doi:10.1097/GCO.0b013e3283409c91
7. Zhang S, Cheng J, Quan C, et al. circCELSR1 (hsa_circ_0063809) Contributes to Paclitaxel Resistance of Ovarian Cancer Cells by Regulating FOXR2 Expression via miR-1252. *Mol Ther Nucleic Acids*. 2020;19:718-730. doi:10.1016/j.omtn.2019.12.005
8. Huang R, Zhu L, Zhang Y; XIST lost induces ovarian cancer stem cells to acquire taxol resistance via a KMT2C-dependent way. Cancer Cell Int. 2020;20(436. doi:10.1186/s12935-020-01500-8
9. Cai Y, Jia R, Xiong H, et al. Integrative gene expression profiling reveals that dysregulated triple microRNAs confer paclitaxel resistance in non-small cell lung cancer via co-targeting MAPT. *Cancer Manag Res*. 2019;11:7391-7404. doi:10.2147/CMAR.S215427
10. Li J, Zheng L, Yan M, et al. Activity and mechanism of flavokawain A in inhibiting P-glycoprotein expression in paclitaxel resistance of lung cancer. *Oncol Lett*. 2020;19(1):379-387. doi:10.3892/ol.2019.11069
11. McCloskey CW, Rodriguez GM, Galpin KJC, Vanderhyden BC. Ovarian Cancer Immunotherapy: Preclinical Models and Emerging Therapeutics. *Cancers (Basel)*. 2018;10(8):244. doi:10.3390/cancers10080244
12. Feng H, Gu ZY, Li Q, Liu QH, Yang XY, Zhang JJ. Identification of significant genes with poor prognosis in ovarian cancer via bioinformatical analysis. *J Ovarian Res*. 2019;12(1):35. doi:10.1186/s13048-019-0508-2
13. Xu Z, Zhou Y, Cao Y, Dinh TL, Wan J, Zhao M. Identification of candidate biomarkers and analysis of prognostic values in ovarian cancer by integrated bioinformatics analysis. *Med Oncol*. 2016;33(11):130. doi:10.1007/s12032-016-0840-y
14. Davis S, Meltzer PS. GEOquery: a bridge between the Gene Expression Omnibus (GEO) and BioConductor. *Bioinformatics*. 2007;23(14):1846-1847. doi:10.1093/bioinformatics/btm254
15. Tang Z, Kang B, Li C, Chen T, Zhang Z. GEPIA2: an enhanced web server for large-scale expression profiling and interactive analysis. *Nucleic Acids Res*. 2019;47(W1):W556-W560. doi:10.1093/nar/gkz430
16. Bardou P, Mariette J, Escudié F, Djemiel C, Klopp C. jvenn: an interactive Venn diagram viewer. *BMC Bioinformatics*. 2014;15(1):293. doi:10.1186/1471-2105-15-293
17. Szklarczyk D, Franceschini A, Wyder S, et al. STRING v10: protein-protein interaction networks, integrated over the tree of life. *Nucleic Acids Res*. 2015;43(Database issue):D447-D452. doi:10.1093/nar/gku1003
18. Liao Y, Wang J, Jaehnig EJ, Shi Z, Zhang B. WebGestalt 2019: gene set analysis toolkit with revamped UIs and APIs. *Nucleic Acids Res*. 2019;47(W1):W199-W205. doi:10.1093/nar/gkz401
19. Gyorffy B, Lánczky A, Szállási Z. Implementing an online tool for genome-wide validation of survival-associated biomarkers in ovarian-cancer using microarray data from 1287 patients. *Endocr Relat Cancer*. 2012;19(2):197-208. doi:10.1530/ERC-11-0329
20. Rhodes DR, Yu J, Shanker K, et al. ONCOMINE: a cancer microarray database and integrated data-mining platform. *Neoplasia*. 2004;6(1):1-6. doi:10.1016/S1476-5586(04)80047-2
21. Vasaikar SV, Straub P, Wang J, Zhang B. LinkedOmics: analyzing multi-omics data within and across 32 cancer types. *Nucleic Acids Res*. 2018;46(D1):D956-D963. doi:10.1093/nar/gkx1090
22. Li T, Fan J, Wang B, et al. TIMER: A Web Server for Comprehensive Analysis of Tumor-Infiltrating Immune Cells. *Cancer Res*. 2017;77(21):e108-e110. doi:10.1158/0008-5472.CAN-17-0307
23. Ru B, Wong CN, Tong Y, et al. TISIDB: an integrated repository portal for tumor-immune system interactions. *Bioinformatics*. 2019;35(20):4200-4202. doi:10.1093/bioinformatics/btz210
24. Link T, Kuhlmann JD, Kobelt D, et al. Clinical relevance of circulating MACC1 and S100A4 transcripts for ovarian cancer. *Mol Oncol*. 2019;13(5):1268-1279. doi:10.1002/1878-0261.12484
25. Nakanishi H, Taccioli C, Palatini J, et al. Loss of miR-125b-1 contributes to head and neck cancer development by dysregulating TACSTD2 and MAPK pathway. *Oncogene*. 2014;33(6):702-712. doi:10.1038/onc.2013.13
26. Parsana P, Amend SR, Hernandez J, Pienta KJ, Battle A. Identifying global expression patterns and key regulators in epithelial to mesenchymal transition through multi-study integration. *BMC Cancer*. 2017;17(1):447. doi:10.1186/s12885-017-3413-3
27. Cheng Y, Mo F, Li Q, et al. Targeting CXCR2 inhibits the progression of lung cancer and promotes therapeutic effect of cisplatin. *Mol Cancer*. 2021;20(1):62. doi:10.1186/s12943-021-01355-1
28. Tamura T, Chiba J. STEAP4 regulates focal adhesion kinase activation and CpG motifs within STEAP4 promoter region are frequently methylated in DU145, human androgen-independent prostate cancer cells. *Int J Mol Med*. 2009;24(5):599-604. doi:10.3892/ijmm_00000270
29. Yang J. Identification of novel biomarkers, MUC5AC, MUC1, KRT7, GAPDH, CD44 for gastric cancer. *Med Oncol*. 2020;37(5):34. doi:10.1007/s12032-020-01362-0
30. Zhang Z, Tu K, Liu F, et al. FoxM1 promotes the migration of ovarian cancer cell through KRT5 and KRT7. *Gene*. 2020;757:144947. doi:10.1016/j.gene.2020.144947